

# Orbital Polarization and Fluctuation in Manganese Oxides

Ryo Maezono and Naoto Nagaosa

Department of Applied Physics, University of Tokyo, Bunkyo-ku, Tokyo 113-8656, Japan  
(October 24, 2018)

## I. INTRODUCTION

Doped manganites  $(R_{1-x}, A_x)_{n+1}\text{Mn}_n\text{O}_{3n+1}$  ( $R=\text{La, Pr, Nd, Sm}$ ;  $A=\text{Ca, Sr, Ba}$ ;  $n=1, 2, \infty$ ) have recently attracted considerable interests due to the colossal magnetoresistance (CMR) observed near the ferromagnetic (spin- $F$ -type) transition temperature  $T_c$ .<sup>1-6</sup> It is now recognized that the most fundamental interaction in these materials is the double exchange interaction, which connects the transport and magnetism.<sup>7-10</sup> Since the discovery of the CMR<sup>3</sup>, however, it has been pointed out that the double-exchange mechanism alone cannot explain not only the CMR<sup>11</sup> but also the several observed properties in this system. As the mechanism which plays an essential role on CMR in cooperate with double-exchange interaction, several candidates has been suggested, for example, the Jahn-Teller (JT) polaron<sup>11-14</sup>, the charge inhomogeneity<sup>15-18</sup>, the percolative processes<sup>19,20</sup>, the phase segregation with respect to the orbital<sup>21</sup>, and the orbital polarization and fluctuation<sup>22-24</sup>, the last of which we describe in this manuscript.

The well-known issue showing the importance of the orbital polarization is the layered ( $A$ -type) antiferromagnetism (AF) observed in the mother compound of this system.<sup>25-27</sup> Kugel and Khomskii<sup>26</sup> treated this in a framework of the superexchange interaction and showed that the full consideration of the orbital degeneracy is indispensable to explain the spin  $A$ -type structure. There the *orbital polarization* is essential: Under the doubly degenerate orbitals, the on-site Coulombic repulsion differs depending on the configuration of the occupation,  $U$  for the two electrons occupying the same orbital,  $U' - J$  for occupying the different orbitals with the parallel spin, and  $U' + J$  for occupying the different orbitals with the anti-parallel spins, where  $U$  and  $U'$  are the intra- and inter-orbital Coulombic interactions, respectively, and  $J$  is the interorbital exchange interaction.<sup>26</sup> In order to maximize the energy gain via the second-order perturbative processes, electrons form the staggered orbital occupation (AF orbital ordering) with the energy gain by  $t^2/(U' - J)$ .<sup>26</sup> In such an orbital ordering, there is a definite distinction between the occupied and unoccupied orbitals, which is the *orbital polarization*. The orbital polarization (or orbital ordering) is the important origin of the  $A$ -type spin structure in the mother compound. In the viewpoint that the CMR with  $x \sim 0.175$ <sup>3</sup> occurs in the lightly doped Mott insulator, the orbital polarization is likely to survive and to play an important role on CMR.

Another point is that the origin of Hund's coupling  $J_H$  is nothing but the on-site Coulomb interactions. It seems therefore rather artificial to take  $J_H \rightarrow \infty$  while the on-site repulsion is neglected, as in the framework of the double-exchange mechanism.<sup>9</sup>

In a form which include the mother compound, we studied the extended Hubbard-type model with the orbital degeneracy for any doping concentration.<sup>23,24</sup> Calculated meanfield phase diagram well reproduced the global topology of the magnetic structure depending on the doping concentration  $x$ .<sup>23,24</sup> With a large orbital polarization we could predict the emergence of the  $A$ -type and the rod-type ( $C$ -type) AF in the moderately doped region, independently from the experiments discovering these phases in the CMR compound with finite  $x$  (which is larger than that for the CMR region)<sup>28-32</sup> It turned out that these phases couldn't be reproduced without a large orbital polarization, which is therefore essential in the doped region where these  $AF$  phases are observed. Because the orbital polarization increases as  $x$  decreases, this concludes that the large orbital polarization survives even in the CMR region with smaller  $x$ . Base on this result, we discuss the spin canting, the spin wave dispersion, and spin wave stiffness from the standing point of the large orbital polarization. We also discuss the orbital fluctuation which turned out to be important in the ferromagnetic metallic (FM) region where the CMR is observed. Spin wave softening near the zone boundary is also discussed in this context.

## II. MODEL AND FORMALISM

We start with the Hamiltonian

$$H = H_K + H_{\text{Hund}} + H_{\text{on site}} + H_S + H_{\text{el-ph}}, \quad (1)$$

where  $H_K$  is the kinetic energy of  $e_g$  electrons,  $H_{\text{Hund}}$  is the Hund's coupling between  $e_g$  and  $t_{2g}$  spins, and  $H_{\text{on site}}$  represents the on-site Coulomb interactions between  $e_g$  electrons.  $t_{2g}$  spins are treated as the localized spins with  $S = 3/2$ . The AF coupling between nearest neighboring  $t_{2g}$  spins is introduced in  $H_S$  to reproduce the NaCl-type ( $G$ -type) AF spin ordering observed at  $x = 1.0$ .<sup>25</sup> Using an operator  $d_{i\sigma\gamma}^\dagger$  which creates an  $e_g$  electron with spin  $\sigma$  ( $= \uparrow, \downarrow$ ) in the orbital  $\gamma$  [ $= a(d_{x^2-y^2}), b(d_{3z^2-r^2})$ ] at site  $i$ , each term of Eq. (1) is given as

$$H_K = \sum_{\sigma\gamma\gamma'\langle ij \rangle} t_{ij}^{\gamma\gamma'} d_{i\sigma\gamma}^\dagger d_{j\sigma\gamma'}, \quad (2)$$

$$H_{\text{Hund}} = -J_H \sum_i \vec{S}_{t_{2g}i} \cdot \vec{S}_{e_g i} , \quad (3)$$

and

$$H_S = J_S \sum_{\langle ij \rangle} \vec{S}_{t_{2g}i} \cdot \vec{S}_{t_{2g}j} . \quad (4)$$

$t_{ij}^{\gamma\gamma'}$  in  $H_K$  is the electron transfer integral between nearest neighboring sites and it depends on the pair of orbitals and the direction of the bond as follows:<sup>27</sup>

$$t_{i\ i+x}^{\gamma\gamma'} = t_0 \begin{pmatrix} -\frac{3}{4} & \frac{\sqrt{3}}{4} \\ \frac{\sqrt{3}}{4} & -\frac{1}{4} \end{pmatrix} , \quad (5)$$

$$t_{i\ i+y}^{\gamma\gamma'} = t_0 \begin{pmatrix} -\frac{3}{4} & -\frac{\sqrt{3}}{4} \\ -\frac{\sqrt{3}}{4} & -\frac{1}{4} \end{pmatrix} , \quad (6)$$

and

$$t_{i\ i+z}^{\gamma\gamma'} = t_0 \begin{pmatrix} 0 & 0 \\ 0 & -1 \end{pmatrix} . \quad (7)$$

$t_0$  is the electron transfer integral between  $d_{3z^2-r^2}$  orbitals along the  $z$  direction. The spin operator for the  $e_g$  electron is defined as  $\vec{S}_{e_g i} = \frac{1}{2} \sum_{\gamma\alpha\beta} d_{i\gamma\alpha}^\dagger \vec{\sigma}_{\alpha\beta} d_{i\gamma\beta}$  with the

Pauli matrices  $\vec{\sigma}$ .  $\vec{S}_{t_{2g}i}$  denotes the localized  $t_{2g}$  spin on the  $i$  site with  $S = 3/2$ .  $H_{\text{on site}}$  consists of the intra- and the inter-orbital Coulomb interactions and the inter-orbital exchange interaction;<sup>24,27</sup>

$$\begin{aligned} H_{\text{on site}} &= U \sum_{j\gamma} n_{j\gamma\uparrow} n_{j\gamma\downarrow} \\ &+ U' \sum_{j\sigma\sigma'} n_{ja\sigma} n_{jb\sigma'} \\ &+ J \sum_{j\sigma\sigma'} d_{ja\sigma}^\dagger d_{jb\sigma'}^\dagger d_{ja\sigma} d_{jb\sigma} \\ &= - \sum_i \left( \tilde{\beta} \vec{T}_i^2 + \tilde{\alpha} \vec{S}_{e_g i}^2 \right) , \end{aligned} \quad (8)$$

where  $n_{j\gamma\sigma} = d_{j\gamma\sigma}^\dagger d_{j\gamma\sigma}$  and  $n_{j\gamma} = \sum_{\sigma} n_{j\gamma\sigma}$ , and the isospin operator describing the orbital degrees of freedom is defined as

$$\vec{T}_i = \frac{1}{2} \sum_{\gamma\gamma'\sigma} d_{i\gamma\sigma}^\dagger \vec{\sigma}_{\gamma\gamma'} d_{i\gamma'\sigma} . \quad (9)$$

Coefficients of the spin and isospin operators, i.e.,  $\tilde{\alpha}$  and  $\tilde{\beta}$ , are given as<sup>24,27</sup>

$$\tilde{\alpha} = U - \frac{J}{2} > 0 , \quad (10)$$

and

$$\tilde{\beta} = U - \frac{3J}{2} > 0 . \quad (11)$$

The magnitude of the meanfield solution of the isospin operator  $\langle \vec{T} \rangle$  gives the energy splitting between the occupied and unoccupied orbitals, namely the *orbital polarization*. Therefore, the minus sign in Eq. (2) means that the on-site repulsion in this system induces not only the spin polarization but also the orbital polarization as the interplay with the orbital degree of freedom. By this orbital polarization, the anisotropy of the  $e_g$  orbitals is fully reflected to the transport and hence introduces the lower dimensionality even in the system with the isotropic crystal structure ( $n = \infty$ ; 113-system). The parameters  $\tilde{\alpha}, \tilde{\beta}, t_0$ , used in the numerical calculation are chosen as  $t_0 = 0.72$  eV,  $U = 6.3$  eV, and  $J = 1.0$  eV, being relevant to the actual manganese oxides.<sup>23,24</sup> The electron-phonon interaction is given as,<sup>24</sup>

$$H_{\text{el-ph}} = +|g| r \sum_i \vec{v}_i \cdot \vec{T}_i , \quad (12)$$

where  $g$  is the coupling constant and  $r$  ( $\vec{v}_i$ ) is the magnitude (direction) of the lattice distortion of the  $\text{MnO}_6$ -octahedra. Values of  $r$  and  $\vec{v}$  are taken from the observed elongation as,  $r \sim 0.028$  and  $\vec{v} = \pm(\sqrt{3}/2)\hat{x} - (1/2)\hat{z}$  (staggered as  $d_{3x^2-r^2}/d_{3y^2-r^2}$ ) for  $\text{LaMnO}_3$  ( $n = \infty$ ),<sup>33</sup> and  $r \sim 0.01$ ,  $\vec{v}/\hat{z}$  (elongation along  $c$ -axis) in  $(\text{La}_{1-x}, \text{Sr}_x)_3\text{Mn}_2\text{O}_7$  ( $0.3 < x < 0.4$ ).<sup>30</sup>

In the path-integral representation, the grand partition function is represented as

$$\Xi = \int \prod_i D\vec{S}_{t_{2g}i} D\bar{d}_{i\gamma\sigma} Dd_{i\gamma\sigma} \exp \left\{ - \int d\tau L(\tau) \right\} , \quad (13)$$

with

$$L(\tau) = H(\tau) + \sum_{\sigma\gamma i} \bar{d}_{i\gamma\sigma}(\tau) (\partial_\tau - \mu) d_{i\gamma\sigma}(\tau) , \quad (14)$$

where  $\tau$  is the imaginary time introduced in the path-integral formalism, and  $\bar{d}_{i\gamma\sigma}$ ,  $d_{i\gamma\sigma}$  are the Grassmann variables corresponding to the operators  $d_{i\gamma\sigma}^\dagger$  and  $d_{i\gamma\sigma}$ , respectively. By introducing two kinds of auxiliary fields corresponding to the following mean-field solutions,<sup>24</sup>

$$\vec{\varphi}_S = \langle \vec{S}_{e_g} \rangle + \frac{J_H}{2\tilde{\alpha}} \langle \vec{S}_{t_{2g}} \rangle , \quad (15)$$

$$\vec{\varphi}_T = \langle \vec{T} \rangle , \quad (16)$$

we obtain the effective action with respect to these auxiliary fields and  $\vec{S}_{t_{2g}}$ , after integrating over the fermion variables as,<sup>24</sup>

$$\Xi = \int D\{\varphi\} e^{S_{\text{eff}}[\vec{\varphi}]} , \quad (17)$$

$$S_{\text{eff}}[\vec{\varphi}] = \text{Tr} \ln G_{kk';nn';\gamma\gamma';\alpha\beta}^{-1} - \int d\tau L_{\vec{\varphi}} , \quad (18)$$

$$L_{\vec{\varphi}} = J_S \sum_{\langle ij \rangle} \vec{S}_{t_{2g}i}(\tau) \cdot \vec{S}_{t_{2g}j}(\tau) - J_H \sum_i \vec{S}_{t_{2g}i}(\tau) \cdot \vec{\varphi}_{Si}(\tau) \\ + \tilde{\alpha} \sum_i \vec{\varphi}_{Si}^2(\tau) + \tilde{\beta} \sum_i \vec{\varphi}_{Ti}^2(\tau) , \quad (19)$$

$$G_{kk';nn';\gamma\gamma';\alpha\beta}^{-1} = (-i\omega_n - \mu) \delta_{kk';nn';\gamma\gamma';\alpha\beta} + M_{kk';nn';\gamma\gamma';\alpha\beta} , \quad (20)$$

$$M_{kk';nn';\gamma\gamma';\alpha\beta} = \varepsilon_k^{\gamma\gamma'} \delta_{kk'} \delta_{nn'} \delta_{\alpha\beta} \\ - \frac{\tilde{\alpha}}{\sqrt{\beta N}} \vec{\sigma}_{\alpha\beta} \cdot \vec{\varphi}_S(k - k', \omega_n - \omega_{n'}) \delta_{\gamma\gamma'} \\ - \frac{\tilde{\beta}}{\sqrt{\beta N}} \vec{\sigma}_{\gamma\gamma'} \cdot \vec{\varphi}_T(k - k', \omega_n - \omega_{n'}) \delta_{\alpha\beta} , \quad (21)$$

where we have introduced the momentum representation,

$$\varphi_{xj}(\tau) = \frac{1}{\sqrt{\beta N}} \sum_k \sum_n \varphi_x(k, \omega_n) e^{i\vec{k} \cdot \vec{R}_j - i\omega_n \tau} , \quad (22)$$

for  $x = S, T$ .

In the meanfield approximation, the free energy is given as

$$F_{MF} = -k_B T \cdot S_{\text{eff}}[\vec{\varphi}^c] + \mu N , \quad (23)$$

where  $\vec{\varphi}^c$  denotes the saddle point of  $\vec{\varphi}_{S,T}$ . We seek the saddle point within the several assumed ordering configurations, as following: We consider four kinds of the spin alignment in the cubic cell: spin  $F$ ,  $A$ ,  $C$  and  $G$  (NaCl-type). For spin  $A$ , we also consider the possibility of the canting characterized by an angle  $\eta$  which is 0 ( $\pi$ ) for spin  $F$  ( $A$ ). As for the double-layered compounds ( $n = 2$ ), we consider an isolated double-layer, for which the Brillouin zone contains only two  $\vec{k}$ -points along  $c$ -axis, because the exchange interaction between two double-layers is reported to be less than 1/100 compared with the intra double-layer one.<sup>34</sup> As for the orbital degrees of freedom, we consider two sublattices  $I$ , and  $II$ , on each of which the orbital is specified by the angle  $\theta_{I,II}$  as<sup>24</sup>

$$|\theta_{I,II}\rangle = \cos \frac{\theta_{I,II}}{2} |d_{x^2-y^2}\rangle + \sin \frac{\theta_{I,II}}{2} |d_{3z^2-r^2}\rangle . \quad (24)$$

We also consider four types of orbital-sublattice ordering, i.e.,  $F$ -,  $A$ -,  $C$ -,  $G$ -type in the cubic cell. Henceforth, we often use a notation such as spin  $A$ , orbital  $G$  ( $\theta_I, \theta_{II}$ ) etc.. Denoting the wave vector of the spin (orbital) ordering as  $\vec{q}_S$  ( $\vec{q}_T$ ), the ground state energy is given as a function of the spin ordering ( $\eta, \vec{q}_S$ ), the orbital ordering ( $\theta_{I,II}, \vec{q}_T$ ), and the lattice distortion ( $g, r, \vec{v}$ ).

In the random-phase-approximation (RPA), we expand  $S_{\text{eff}}[\vec{\varphi}]$  with respect to the small fluctuation  $\delta\vec{\varphi}_S$  from its mean-field solution  $\vec{\varphi}_S^c$  for the spin degrees of freedom,

$$\vec{\varphi}_S = \vec{\varphi}_S^c + \delta\vec{\varphi}_S . \quad (25)$$

Denoting the perpendicular (parallel) component to the mean-field as  $\vec{\pi}$  ( $\vec{\sigma}$ ),

$$\delta\vec{\varphi}_S(k, \omega_n) = \vec{\sigma}(k, \omega_n) + \vec{\pi}(k, \omega_n) , \quad (26)$$

the deviation of the action can be written as<sup>35</sup>

$$\delta S_{\text{eff}} = \sum_{q, \Omega} K_{\pi}(\vec{q}, \Omega) \pi(\vec{q}_S + \vec{q}, \Omega) \cdot \pi(-\vec{q}_S - \vec{q}, -\Omega) \\ + \sum_{q, \Omega} K_{\sigma}(\vec{q}, \Omega) \vec{\pi}(\vec{q}_S + \vec{q}, \Omega) \cdot \{\vec{n} \times \vec{\pi}(-\vec{q}_S - \vec{q}, -\Omega)\} . \quad (27)$$

Because the spin wave is the Goldstone boson, the condition  $K_{\pi}(0, 0) = 0$ ,  $K_{\sigma}(0, 0) = 0$ , can be derived. Coefficient of the diagonalized quadratic form is obtained as  $K_{\uparrow(\downarrow)} = K_{\pi} \pm iK_{\sigma}$ , zero-point of which ( $K_{\uparrow(\downarrow)}(\vec{q}, \Omega = -i\omega) = 0$ ) gives the dispersion relation of the excitation  $\omega = \omega(\vec{q})$ .  $K_{\sigma}(\vec{q}, \Omega)$  can be expanded as,

$$\frac{K_{\sigma}(\vec{q}, \Omega)}{\tilde{\alpha}} = \begin{cases} \sigma A \cdot i\Omega + \sum_{\alpha=x,y,z} C_{\alpha} q_{\alpha}^2 & \cdots \text{Spin } F \\ B\Omega^2 + \sum_{\alpha=x,y,z} C_{\alpha} q_{\alpha}^2 & \cdots \text{Spin } AF \end{cases} , \quad (28)$$

where  $\sigma = 1$  ( $-1$ ) corresponds to spin up (down), respectively. We evaluate only the *static* spin-wave stiffness  $C_{\alpha} = C_{\alpha}(x)$  because the *dynamic* spin wave velocity evaluated by using the above expression inherently gives a misleading estimation; For the half-filled insulator,  $x = 0$ , it does not reduce to the energy order as the superexchange interaction  $\sim t^2/U$ , giving rather the order of  $t$ ,<sup>36</sup> perhaps due to the inherent fault of the RPA. For the metallic region,  $x \neq 0$ , we cannot reproduce the correct dispersion-relation, because the Landau-damping is not properly treated in our calculation where the Brillouin zone is discretized and thus the gapless individual-excitation is not correctly evaluated.  $C_{\alpha} = C_{\alpha}(x)$  roughly reflects the exchange-interaction depending on  $x$ .

### III. ORBITAL POLARIZATION AND FLUCTUATION

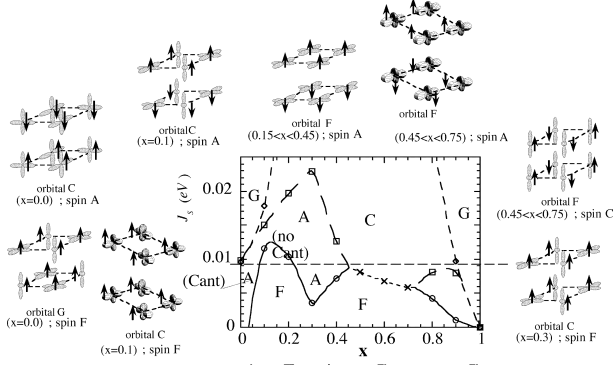


FIG. 1. Mean field phase diagram as a function of the carrier concentration ( $x$ ) and the antiferromagnetic interaction between  $t_{2g}$  spins ( $J_S$ ) for the cubic system ( $n = \infty$ ; 113-system).<sup>23,24</sup> Dotted line ( $J_S = 0.009$ ) well reproduces the change of the spin structure experimentally observed.

Fig. 1 shows the zero-temperature meanfield phase diagram of the cubic system ( $n = \infty$ ; 113-system) in a plane of  $x$  and  $J_S$  (AF superexchange interaction between  $t_{2g}$  spins), with the optimization of the orbital at each point on the plane.<sup>23,24</sup> With  $J_S$  being fixed to be a relevant value to the actual compounds,  $J_S = 0.009$ ,<sup>27,37</sup> we obtain the spin transition as  $A \rightarrow F \rightarrow A \rightarrow C \rightarrow G$  with increasing  $x$ , being consistent with experiments<sup>29</sup>. Non-monotonic phase boundaries are essential for these variety of the spin structures.

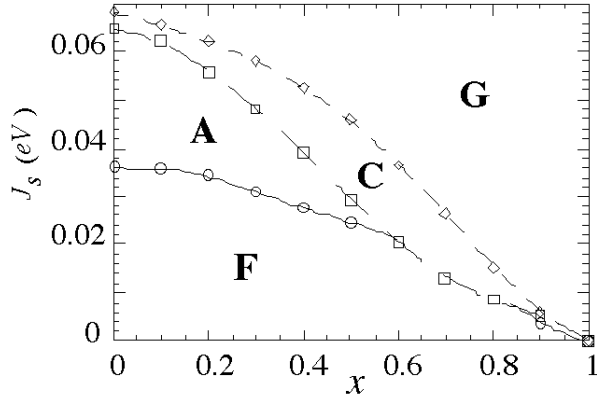


FIG. 2. Mean field phase diagram with no orbital polarization. In this case the nonmonotonic behavior of the phase boundaries disappears.

Dimensionality control by the orbital polarization is the origin of such a behavior: Orbital ordering changes from that maximizing the superexchange energy gain for smaller  $x$  ( $\leq 0.3$ ) to that maximizing the double-exchange energy gain for larger  $x$ , with the change in the dimensionality.<sup>24</sup> This orbital transition varies the

kinetic energy gain non-monotonically via the change in the density of states with the van-Hove singularity.<sup>24</sup> This can also be an origin of the instability toward the phase segregation,<sup>15-18,21</sup> though it does not occur in our calculation.

With no orbital polarization, such a non-monotonic behavior cannot be reproduced,<sup>24</sup> as shown in Fig. 2. This is because the anisotropy of the degenerate orbitals are mixed to disappear with no polarization (in this case we cannot say which orbital is occupied because of the hybridization).

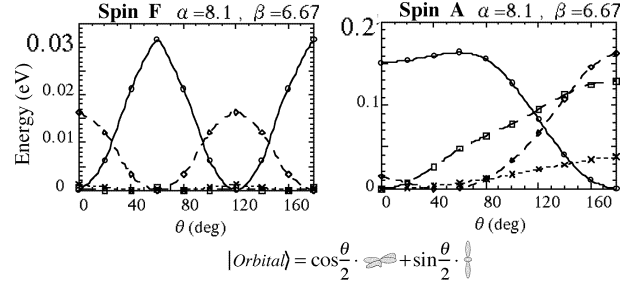


FIG. 3. The energy as a function of the orbital state characterized by  $\theta$  in the several value of  $x$ . (a) Spin  $F$  is assumed. (b) Spin  $A$  is assumed.<sup>24</sup> In both cases, the orbital  $F$ -type structure is assumed.

For the global topology  $A \rightarrow F \rightarrow A \rightarrow C \rightarrow G$  to be reproduced, it is therefore necessary that a large orbital polarization occurs even in the spin  $F$  phase where CMR is observed. As for the spin  $F$  (CMR) phase, however due to its isotropy, the question is how does it coexist with the observed isotropic properties in CMR compounds,<sup>3,55</sup> because such a polarization leads to the anisotropic carrier hopping. The key for this question is the orbital fluctuation.

Fig. 3 shows the energy dependence on the orbital configuration for spin  $F$  and  $A$  phases.<sup>24</sup> In spin  $F$  phase, there are many degenerate saddle points due to the isotropy, and the height of the barrier is an order smaller than that for the  $AF$  phase.

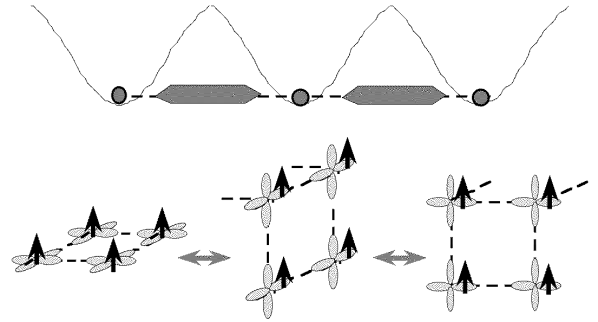


FIG. 4. Schematic picture of the orbital liquid state.

This result implies that the orbital fluctuation becomes

important in the spin  $F$  phase comparing with the  $AF$  phases. Reentrant of the spin  $A$  with increasing  $x$ , seen in Fig. 1 implies that the  $d_{x^2-y^2}$  orbital ordering is inherent property of the double-exchange interaction. Therefore, in the extent beyond the mean field theory, it is likely that the degenerate saddle points,  $d_{x^2-y^2}$ ,  $d_{y^2-z^2}$ , and  $d_{z^2-x^2}$  resonate to recover the isotropy of the spin  $F$  metallic phase though the large orbital polarization still survives, forming the *orbital liquid* state, as shown in Fig. 4.<sup>22</sup>

#### IV. SPIN CANTING AND ORBITAL ORDERING

Fig. 5 shows the phase diagram of the layered compounds ( $n = 2$ ; 327-system).<sup>35</sup> In this system, the anisotropic crystal structure also controls the dimensionality: restricted hopping along  $c$ -axis brings about the  $d_{x^2-y^2}$ -orbital ordering in the metallic region even for the isotropic spin  $G$ - and  $F$  ( $x > 0.2$ ) alignment. Especially the planer spin  $F$  phase seen for  $x > 0.2$  is essential for the spin canting observed in this system<sup>38-43</sup> with  $0.4 \leq x_{exp.} \leq 0.48$ , as below. The global topology of the phase diagram in this system is reproduced as  $A \rightarrow F \rightarrow A \rightarrow G$  with increasing  $x$ ,<sup>44</sup> as shown in Fig. 5, where there are two phase boundaries between the spin  $A$  and  $F$  phases; One is with small  $x$  ( $x < 0.1$ , *left* boundary), and the other is with finite  $x$  ( $x > 0.1$ , *right* boundary). Under the competition between the super- and double-exchange interaction, the saddle point of the canting angle  $\eta$  is given as,<sup>35</sup>

$$\cos \frac{\bar{\eta}}{2} = \frac{t_z x}{4J_S}, \quad (29)$$

where the  $t_z$  denotes the inter-layer hopping integral.

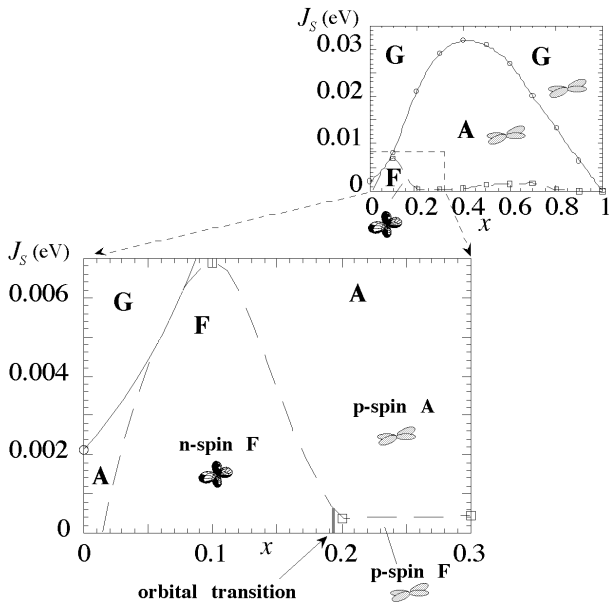


FIG. 5. Phase diagram for the layered compounds ( $n = 2$ ; 327-system).<sup>35</sup>

The right-hand-side of the above equation should be smaller than the unity for the occurrence of the spin canting. For the *left* boundary, this condition can be satisfied for any magnitude of  $t_z$  because the small  $x$  always makes the right-hand-side of Eq. (29) to be small. For the *right* boundary, however, this can be satisfied only when the orbital is planer, i.e., nearly  $d_{x^2-y^2}$  with small  $t_z$ ; the characteristic energy scale of the hopping integral is an order greater than that for  $J_S$ , therefore if the orbital is spherical,  $t_z/J_S$  becomes much more than the unity and hence the right-hand-side of Eq. (29) because in this case the finite  $x$  does not make it small any more. Therefore it is concluded that the planer orbital is indispensable for the canting observed on the *right* phase boundary with finite  $x$  (metallic canting).

Experimentally, this metallic canting is commonly found in the double-layered compound ( $n = 2$ ).<sup>38-43</sup> This is because the layered structure stabilizes the planer ( $d_{x^2-y^2}$ ) orbital in the metallic region. In the 113-system, on the other hands, no spin canting on the *right* boundary is reported,<sup>28</sup> which may be accounted by its isotropy leading to no such stabilization. This isotropy of the 113-compounds may allow only two possibilities for its orbital state; one is the orbital liquid state resonating among the planer orbitals,  $d_{x^2-y^2}$ ,  $d_{y^2-z^2}$ , and  $d_{z^2-x^2}$ ,<sup>22</sup> and the other is the quasi-spherical orbital, which is obtained as the saddle point within the extent of the meanfield theory, as shown in Fig. 1.<sup>23,24</sup> Kawano *et al.* observed the metallic canting in 113-system,  $\text{Nd}_{1/2}\text{Sr}_{1/2}\text{MnO}_3$ , with slight anisotropy of the lattice structure<sup>45</sup> in the temperature-driven transition between the spin  $F$  (high-temperature phase) and the spin  $A$  (low-temperature phase). This supports the former possibility of the orbital, i.e., the orbital liquid state; If the orbital is quasi-spherical in perfectly cubic system, taking the latter possibility, such a slight lattice anisotropy leads to only a slight distortion of the spherical orbital which remains the right-hand-side of Eq. (29) still larger than the unity and hence no canting is expected. On the other hand, taking the former possibility, such a slight anisotropy is enough to stabilize  $d_{x^2-y^2}$  immediately and hence the metallic canting can be explained.

Another important feature as for the metallic canting is the stability of the spin  $A$  phase against the canting. When the  $x$  holes are introduced, the kinetic energy gain  $\Delta E_{kin}(\xi)$  via the bonding and anti-bonding splitting  $\Delta = t_z \cos \frac{\eta}{2} = t_z \xi$ .<sup>9</sup> is given as,<sup>35</sup>

$$\Delta E_{kin}(\xi) \sim \begin{cases} -t_z^2 \cdot N_F \cdot \xi^2 & (\text{for } \xi < \xi_c \equiv \frac{x}{N_F t_z}) \\ -t_z \cdot x \cdot \xi & (\text{for } \xi > \xi_c) \end{cases}, \quad (30)$$

with simplifications of a perfect spin polarization and the constant density of states. The competition between this kinetic energy gain and the energy cost of the exchange interaction,  $J_S \cos \eta = J_S (2\xi^2 - 1)$ , is the origin of the spin canting. The lower line of Eq. (30) is obtained by de Gennes, and if this holds the canting always occurs.<sup>10</sup> The new aspect here is that  $\Delta E_{kin}(\xi) \propto \xi^2$

when the splitting  $\Delta = t_z \xi$  is smaller than the Fermi energy  $\epsilon_F = x/N_F$  and both the bonding and anti-bonding bands are occupied. Therefore the spin A structure ( $\xi = 0$ ,  $\eta = \pi$ ) is at least locally stable when  $2J_S > t_z^2 N_F$ . This condition can be satisfied when the orbital is almost  $d_{x^2-y^2}$  and  $t_z$  is much reduced from  $t_0$ . By minimizing the total energy  $\Delta E(\xi) = \Delta E_{kin}(\xi) + \Delta E_{ex}(\xi)$ , it is found that the spin canting can occur only when  $\xi_c < 1$ ; When  $\xi_c > 1$  ( $x > t_z N_F$ ), only the upper line of Eq. (30) is relevant and  $\Delta E = (2J_S - t_z^2 N_F) \cdot \xi^2$ . Therefore  $\xi$  jumps from 1 (spin F) to 0 (spin A) as  $J_S$  increases across  $t_z^2 N_F/2$ .

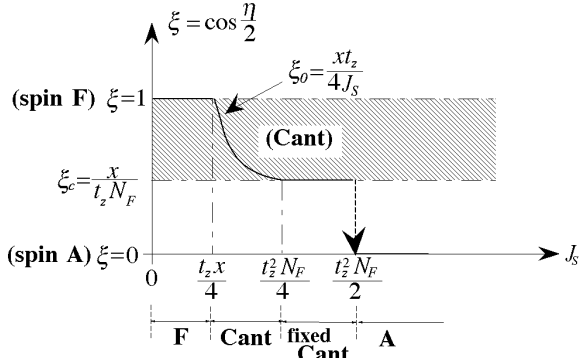


FIG. 6. the optimized  $\xi$  as a function of  $J_S$  for the case  $\xi_c < 1$ .<sup>35</sup>

When  $\xi_c < 1$  (the spin canting can occur), the optimized  $\xi$  as a function of  $J_S$  is given in Fig. 6. As  $J_S$  increases, the spin structure changes as spin F ( $J_S < t_z x/4$ )  $\rightarrow$  spin canting ( $t_z x/4 < J_S < t_z^2 N_F/4$ )  $\rightarrow$  spin canting with fixed canting angle ( $t_z^2 N_F/4 < J_S < t_z^2 N_F/2$ )  $\rightarrow$  spin A ( $t_z^2 N_F/2 < J_S$ ). Note that the canting angle continuously evolves from spin F, but jumps at the transition to the spin A. This seems to be consistent with experiments<sup>43</sup> where the canting angle larger than 63 deg. is not observed.

## V. SPIN DYNAMICS AND ORBITAL

By fitting  $K_\sigma(\vec{q}, 0)$  as a function of  $\vec{q}$ , in Eq. (28), we can evaluate the *static* stiffness of the spin wave excitation  $C_\alpha$  due to the  $e_g$  orbital contribution. As the orbital configurations to be assumed, we take the saddle-point solution obtained in the meanfield theory as,<sup>23,24</sup>

$x = 0.0$	Spin A	Orbital C:(60, -60)
$x = 0.1$	Spin F	Orbital C:(80, -80)
$x = 0.2 - 0.4$	Spin A	Orbital F:(0,0)
$x = 0.5 - 0.9$	Spin C	Orbital F:(180,180).

As for  $x = 0$ , we further introduced the JT effect<sup>24</sup> by putting the observed distortion of the  $\text{MnO}_6$  octahedra.<sup>33</sup> Fig. 7 shows the  $q$ -dependence of  $-K_\downarrow(q_x, 0)$  for the

spin A configuration with  $d_{x^2-y^2}$  orbital ordering (Minus sign of  $K_\downarrow$  comes from the negative  $B$  in Eq. (28) to correspond the positive sign of the plot with the stability of the saddle point).

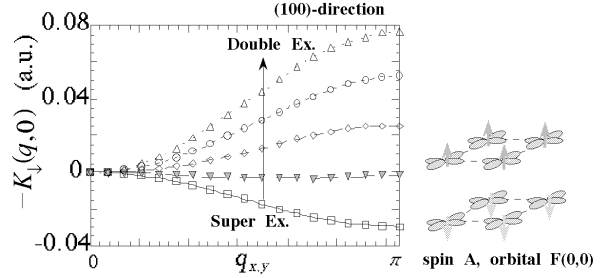


FIG. 7. wave vector dependence of  $-K_\downarrow(q_x, 0)$  calculated for the spin A,  $d_{x^2-y^2}$  orbital ordering, as an example. Minus sign of  $K_\downarrow$  comes from the negative  $B$  in Eq. (28) to correspond the positive sign of the plot with the stability of the saddle point.

We have chosen this structure, as an example, because the double exchange interaction is most effective in this ordering as the meanfield theory shows,<sup>24</sup> and hence the crossover from super- to double-exchange manifests itself most remarkably. The enhancement of the stiffness with increasing  $x$  can be reproduced. This is due to the crossover from the super- to the double-exchange interaction as  $x$  increases, which is well evaluated in our formalism in the unified way, as the inter- and intra-band transitions, respectively. Plots are well fitted in the whole Brillouin zone for the ferromagnetic-bond direction by

$$-K_\downarrow(\vec{q}, 0) \propto (1 - \cos q_\alpha), \quad (31)$$

not only in this case but also for all the other ordering shown in the above table. This implies that only the nearest-neighbor interactions are important in the spin wave excitation. This issue is important because there is no guarantee that the exchange interaction can be represented by the nearest neighbor Heisenberg model at finite doping, and because the softening near the zone boundary has been observed in some materials experimentally.<sup>46-49</sup> Our result here is in sharp contrast to the first principle study<sup>50</sup> which attributes the origin of such a softening to the longer-range interactions than the nearest-neighbor interactions. Negative stiffness  $C_\alpha < 0$  seen for  $x = 0$ , (100)-direction, corresponds to the instability of the spin structure, which can be explained as follows. Around  $x = 0$  the spin structure is dominated by the superexchange interaction where the energy gain for spin-F (AF) bond is  $t_{o-u}^2 / \tilde{\beta}$  ( $t_{o-o}^2 / \tilde{\alpha}$ ),<sup>24</sup> where  $t_{o-o}$  ( $t_{o-u}$ ) are the transfer integral between the nearest-neighboring occupied/occupied (occupied/unoccupied) orbitals. Orbital F (0,0) leads to  $t_{o-o}^{x,y} > t_{o-u}^{x,y}$  and thus the intra-plane bonds favor spin-AF for our choice of the parameters  $\tilde{\alpha} \approx \tilde{\beta}$ . This destabilizes the spin A structure in (100)-direction. As the doping  $x$  increases, the double-exchange interaction, becomes more and more important.

This stabilizes the ferromagnetic bond within the plane, and  $C_{x(y)}$  becomes positive.

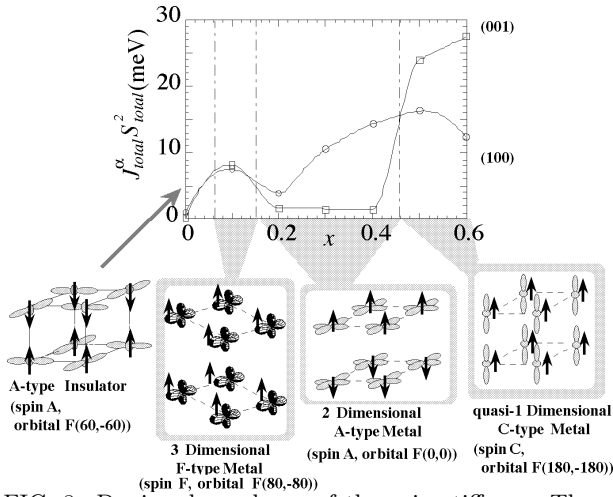


FIG. 8. Doping-dependence of the spin stiffness. The orbital and the spin structure are optimized at each point. The enhancement of the spin-stiffness and the cross-over of the dimensionality are seen with increasing  $x$ .<sup>53</sup>

Fig. 8 shows the *static* spin wave stiffness as a function of the doping concentration  $x$ , including the contribution from  $t_{2g}$  ( $J_S$ ). We could reproduce the qualitative feature of the dimensional crossover and the enhancement<sup>54</sup> of the stiffness in terms of the crossover from the super- (for smaller  $x$ ) to the double-exchange interactions (for larger  $x$ ) accompanied with the change in the orbital ordering. As  $x$  increases, the spin structure changes from spin  $A$  insulator at  $x = 0$  into the nearly isotropic spin  $F$  metal, to the spin  $A$  metal with two-dimensional  $d_{x^2-y^2}$ -orbital alignment, and to the spin  $C$  metal with  $d_{3z^2-r^2}$ -orbital.<sup>23,24</sup> Accordingly, the in-plane stiffness shows an increase, moderately at the beginning and then rapidly in the region of the spin  $A$ -metal. This reflects the fact that the double-exchange interaction is the most effective and prefers the  $d_{x^2-y^2}$ -orbital, i.e., the double-exchange interaction is basically *two-dimensional* with the  $e_g$ -orbitals. In the spin  $C$  metal for  $x > 0.4$ , one-dimensional orbital along (001)-direction gives rise to a steep increase of the stiffness in this direction.

The observed anisotropy of the spin stiffness is determined by the long range ordering of the orbitals. Fig. 8 also represents the cross-over of the dimensionality which we proposed in the previous report.<sup>24</sup> The stiffness changes from the nearly isotropic one in the spin  $F$  state to the considerably strong two-dimensional one for spin  $A$  metal, and to a quasi-one-dimensional one for spin  $C$ , reflecting the orbital transition with increasing  $x$ . Yoshizawa *et al.*<sup>52</sup> observed such two-dimensional anisotropy of the stiffness for  $\text{Nd}_{0.45}\text{Sr}_{0.55}\text{MnO}_3$ , being consistent with our result. Quasi-one-dimensional anisotropy is predicted for  $\text{Nd}_{1-x}\text{Sr}_x\text{MnO}_3$  ( $x > 0.6$ )<sup>31,32</sup>.

The in-plane spin stiffness  $J_{\text{total}}^{x(y)} S_{\text{total}}^2$  in Fig. 8 could be compared with the experiments. In  $\text{La}_{1-x}\text{Sr}_x\text{MnO}_3$ , Endoh *et al.*<sup>54</sup> observed the plateau of the velocity  $v_x$  in the orbital-ordered insulating state up to  $x \sim 0.12$  and then the velocity increases in the spin  $F$  metallic phase. Comparing this with the calculation above, it seems that the moderate increase up to  $x \sim 0.15$  in Fig. 8 corresponds to the plateau, while the rapid increase for  $x > 0.15$  to the increasing velocity observed by Endoh.<sup>54</sup> Then orbital-ordered spin  $F$  metallic state in Fig. 8 corresponds to the insulating spin  $F$  phase in experiments. Both the spin  $F$ - and  $A$ -metal in experiments, on the other hand, seems to corresponds to the spin  $A$ -metal with  $d_{x^2-y^2}$  orbital ordering in the calculation. This fits well orbital liquid picture by Ishihara *et al.*<sup>22</sup>; In the perfectly cubic system the orbital state in spin  $F$  metal is described as the resonance among  $d_{x^2-y^2}$ ,  $d_{y^2-z^2}$ , and  $d_{z^2-x^2}$ . In the actual CMR compound, however, the slight lattice distortion<sup>47,55</sup> may breaks the cubic symmetry to stabilize  $d_{x^2-y^2}$ , though it is still accompanied with large fluctuation around it.

Now we turn to the absolute value of the stiffness in the spin  $F$  metallic phase. Taking the reported lattice constant and the magnitude of spin moment as,  $S^* = 3/2 + 1/2(1-x)$ , the experimental values of the *static* spin stiffness,  $J_{\text{total}}^x S_{\text{total}}^2$ , are 11.61 meV for  $\text{La}_{0.7}\text{Sr}_{0.3}\text{MnO}_3$ <sup>55</sup> and 10.24 meV for  $\text{Nd}_{0.7}\text{Sr}_{0.3}\text{MnO}_3$ <sup>47</sup>, respectively. These are in quite well coincidence with  $J_{\text{total}}^x S_{\text{total}}^2 = 10.53$  meV, estimated by RPA here with  $x = 0.3$ ,  $d_{x^2-y^2}$ -orbital ordering. A simple tight-binding estimation of the static spin stiffness,

$$D = \frac{S^*}{2} \frac{\partial}{\partial(q^2)} \sum_{\langle ij \rangle, \sigma} t_{ij} \langle 0 | c_{i\sigma}^\dagger c_{j\sigma} | 0 \rangle, \quad (32)$$

with  $d_{x^2-y^2}$ -orbital also gives the similar value,  $\sim 10$  meV (with  $t_0 = 0.72$  eV,  $x = 0.3$ ), where the strong Coulombic interactions are reflected as the full orbital polarization  $d_{x^2-y^2}$  (superexchange interactions are ignored). This agreement can be understood in terms of the above orbital liquid picture as follows: While the large orbital fluctuation around  $d_{x^2-y^2}$  may cause the several anomalous behaviors in the transport properties, it is not reflected to the stiffness constant because the correction due to such a fluctuation has the wave vector dependence as  $\sim (1 - \cos q_\alpha)$ <sup>256</sup> as described in the next paragraph, doing little around  $\vec{q} = 0$  and hence the stiffness constant. Therefore the  $d_{x^2-y^2}$ -orbital ordering can give a good estimation of the stiffness constant of spin  $F$  metallic phase with a large orbital fluctuation.

The softening observed near the zone boundary of the spin wave excitation can be understood in terms of the orbital fluctuation.<sup>56</sup> When the normal vector of the resonating planer orbitals,  $d_{x^2-y^2}$ ,  $d_{y^2-z^2}$ , and  $d_{z^2-x^2}$ , points along some bond direction, the ferromagnetic double-exchange interaction disappears along this bond resulting, instead, the  $AF$  interaction due to  $t_{2g}$  orbitals. Such an interaction between the orbital fluctu-

ation and spin degrees of freedom leads to, in the lowest order, the self-energy correction with the  $k$ -dependence as  $\sim (1 - \cos q_\alpha)^2$  for  $(0, 0, \xi)$ - and  $(0, \xi, \xi)$ -direction but no (canceled out) correction for  $(\xi, \xi, \xi)$ <sup>57</sup>, being consistent with the experiments<sup>46</sup>.

The important implication concluded from the agreement between the experimental and RPA-estimated value of the stiffness constant is little influence of the JT polaron,<sup>11–14</sup> at least on the spin dynamics. JT polaron should reduce the double-exchange interaction in the doped region via a bandwidth reduction. To describe this polaronic effect, we introduce here a generic model; Assume that the orbital configuration is relaxed to its stable one when the electron is occupying the site  $i$ . We express the polaronic degrees of freedom by the bosons. Now the electron operators  $d^\dagger, d$  have no orbital index, because of the sufficient orbital polarization,

$$H = \sum_{ij,\sigma} t_{ij} d_{i\sigma}^\dagger d_{j\sigma} + \sum_{i,\sigma} \sum_q g_q (b_q + b_{-q}^\dagger) d_{i\sigma}^\dagger d_{i\sigma} + \sum_k \omega_k b_k^\dagger b_k + U \sum_i n_{i\uparrow} n_{i\downarrow}. \quad (33)$$

This is the usual polaron Hamiltonian, and the following unitary transformation  $\tilde{U}$  eliminates the coupling terms between electrons and bosons,

$$\tilde{U} = \exp \left[ \sum_{i,\sigma} \sum_q \left( \frac{g_q}{\omega_q} \right) n_{i\sigma} e^{iq \cdot R_i} (b_q - b_{-q}^\dagger) \right]. \quad (34)$$

In terms of this  $\tilde{U}$ , the Hamiltonian  $H$  is transformed as<sup>58</sup>

$$\begin{aligned} \tilde{H} &= \tilde{U}^\dagger H \tilde{U} \\ &= \sum_{ij,\sigma} t_{ij} X_i^\dagger X_j d_{i\sigma}^\dagger d_{j\sigma} + \sum_q \omega_q b_q^\dagger b_q \\ &\quad - \sum_{i\sigma} \Delta \cdot n_{i\sigma} + U \sum_i n_{i\uparrow} n_{i\downarrow}, \end{aligned} \quad (35)$$

where  $X_i = \exp[\sum_q e^{iq \cdot R_i} (g_q/\omega_q) (b_q - b_{-q}^\dagger)]$ , and  $\Delta = \sum_q g_q^2/\omega_q$  is the relaxation energy. We now derive the exchange interaction between spins in terms of the perturbative expansion in  $t_{ij}$ . The double-exchange interaction is the first order in  $t_{ij}$ , and is reduced by the factor of  $\langle X_i^\dagger X_j \rangle = \exp[-\sum_q |u_q|^2/2]$  ( $u_q = (g_q/\omega_q)(e^{iq \cdot R_i} - e^{iq \cdot R_j})$ ), which is exponentially small when  $g_q/\omega_q$  is large. This factor is nothing but the bandwidth reduction factor due to the polaronic effect. On the other hand, for  $x = 0$ , the superexchange interaction under the coupling with the polaron is given by,

$$J = 4|t_{ij}|^2 \int_0^\beta d\tau G_0^2(\tau) \langle X_i^\dagger(\tau) X_j(\tau) X_j^\dagger(0) X_i(0) \rangle, \quad (36)$$

where  $G_0(\tau) = e^{-U\tau/2}$  is the Green's function for localized electrons. Because we are interested in the large

$U$  case, the integral is determined by the small  $\tau$  region where  $\langle X_i^\dagger(\tau) X_j(\tau) X_j^\dagger(0) X_i(0) \rangle \cong e^{-\tilde{\Delta}\tau}$  ( $\tilde{\Delta} = \sum_q \omega_q |u_q|^2$ ). Then the polaronic effect is to replace  $U$  by  $U + \tilde{\Delta}$  in the expression for  $J$ , which is a minor correction when  $U \gg \tilde{\Delta}$ <sup>59</sup>, being in sharp contrast to the double-exchange interaction discussed above. Polaronic effect should therefore correct the RPA-estimation of the stiffness-enhancement as  $x$  increases to be smaller. Agreement between the observed and estimated stiffness in the doped region implies therefore that the spin dynamics is not so affected by the JT polaron. This is also pointed out by Quijada *et al.*<sup>60</sup>

Because the estimation is made under the assumption that the orbital is almost fully polarized to  $d_{x^2-y^2}$ , the agreement also suggests the large orbital polarization. With the absence of the orbital polarization, the stiffness enhancement should scale to electron density  $(1-x)$  rather than the hole  $x$ . The observed stiffness enhancement with increasing  $x$  even in the metallic region therefore also supports the large orbital polarization.

## VI. CONCLUSIONS

We discussed the zero-temperature phase diagram and the spin dynamics of the CMR compounds based on the model with a large orbital polarization. The topology of the magnetic transition depending on the doping concentration cannot be reproduced without a large orbital polarization. This is because the double-exchange interaction is the most effective and prefers the  $d_{x^2-y^2}$ -orbital, i.e., the double-exchange interaction is basically *two-dimensional* with the orbital polarization. As for the ferromagnetic metallic phase the large orbital polarization recovers the isotropy of the transport by forming a liquid state, i.e., the resonance among  $d_{x^2-y^2}$ ,  $d_{y^2-z^2}$  and  $d_{z^2-x^2}$ . Spin  $A$  phase seen in the moderately doped region has a stability against the canting with infinitesimal angle deviation from  $\pi$ , being in sharp contrast to the spin  $A$  insulator. Though it cannot be infinitesimal, finite canting angle between  $0$  (spin  $F$ ) and  $\pi$  (spin  $A$ ) can realize only if the orbital is planar both in spin  $F$  and  $A$ . The observed metallic canting in 113-compounds is therefore an evidence that the ferromagnetic metallic phase consists of such a planar orbital. The dispersion of the spin wave excitation evaluated in the RPA is well fitted by the cosine curve. This implies that the excitation is almost dominated by the nearest-neighbor exchange interaction even in the double-exchange regime, being in conflict with the first principle result. Estimated stiffness constant shows good agreement with the observed values for the metallic region. This strongly implies the absence of the JT-polaronic influence on the spin dynamics in the doped region. Based on the above orbital liquid picture, we could explain the spin wave softening near the zone boundary, its anisotropy, and no influence due to the orbital fluctuation on the stiffness constant.



## VII. ACKNOWLEDGEMENT

The authors would like to thank S. Ishihara, S. Maekawa, K. Hirota, Y. Endoh, I. Solov'yev, K. Terakura, T. Kimura, H. Kuwahara, R. Kajimoto, H. Yoshizawa, T. Akimoto, Y. Moritomo, D. Khomskii, A.J. Millis, E.W. Plummer, J.F. Mitchell and Y. Tokura for their valuable discussions. This work was supported by Priority Areas Grants from the Ministry of Education, Science, Sports and Culture of Japan. R.M. is supported by Research Fellowships of the Japan Society for the Promotion of Science (JSPS) for Young Scientists.

- 
- <sup>1</sup> K. Chahara, T. Ohono, M. Kasai, Y. Kanke, and Y. Kozono, Appl. Phys. Lett. **62**, 780 (1993).
  - <sup>2</sup> R. von Helmolt, J. Wecker, B. Holzapfel, L. Schultz, and K. Samwer, Phys. Rev. Lett. **71**, 2331 (1993).
  - <sup>3</sup> Y. Tokura, A. Urushibara, Y. Moritomo, T. Arima, A. Asamitsu, G. Kido, and N. Furukawa, J. Phys. Soc. Jpn. **63**, 3931 (1994), and A. Urushibara, Y. Moritomo, T. Arima, A. Asamitsu, G. Kido and Y. Tokura, Phys. Rev. B **51**, 14103 (1995).
  - <sup>4</sup> S. Jin, T. H. Tiesel, M. McCormack, R. A. Fastnacht, R. Ramesh, and L. H. Chen, Science, **264**, 413 (1994).
  - <sup>5</sup> R.A. Ram, P. Ganguly, and C.N. Rao, J. Solid State Chem. **70**, 82 (1987).
  - <sup>6</sup> Y. Moritomo, Y. Tomioka, A. Asamitsu, Y. Tokura, and Y. Matsui, Phys. Rev. B **51**, 3297 (1995); Y. Moritomo, A. Asamitsu, H. Kuwahara, and Y. Tokura, Nature **380**, 141 (1996).
  - <sup>7</sup> G. H. Jonker, and H. van Santen, Physica **16**, 337 (1950).
  - <sup>8</sup> C. Zener, Phys. Rev. **82**, 403 (1951).
  - <sup>9</sup> P. W. Anderson, and H. Hasegawa, Phys. Rev. **100**, 675 (1955).
  - <sup>10</sup> P. G. de Gennes, Phys. Rev. **118**, 141 (1960).
  - <sup>11</sup> A.J. Millis, P.B. Littlewood and B.I. Shraiman, Phys. Rev. Lett. **74**, 5144 (1995).
  - <sup>12</sup> H. Röder, Jun Zang, and A.R. Bishop, Phys. Rev. Lett. **76**, 1356 (1996).
  - <sup>13</sup> A.J. Millis, B.I. Shraiman and R. Mueller, Phys. Rev. Lett. **77**, 175 (1995).
  - <sup>14</sup> A.S. Alexandrov and A.M. Bratlovsky, Phys. Rev. Lett. **82**, 141 (1999).
  - <sup>15</sup> S. Yunoki, J. Hu, A. L. Malvezzi, A. Moreo, N. Furukawa, and E. Dagotto, Phys. Rev. Lett. **80**, 845 (1998).
  - <sup>16</sup> S. Yunoki and A. Moreo, Phys. Rev. B **58**, 6403 (1998).
  - <sup>17</sup> S. Yunoki, A. Moreo, and E. Dagotto, Phys. Rev. Lett. **81**, 5612 (1998).
  - <sup>18</sup> A. Moreo, S. Yunoki and E. Dagotto, Science **283**, 2034 (1994).
  - <sup>19</sup> J.H. Jung, K.H. Kim, H.J. Lee, J.S. Ahn, N.J. Hur, and T.W. Noh, preprint (cond-mat/9809107).
  - <sup>20</sup> S.W. Cheong, the epitome of the 1999 APS Centennial Meeting, also the abstract of FSRC (1999).
  - <sup>21</sup> Y. Endoh, K. Hirota, S. Ishihara, S. Okamoto, Y. Murakami, A. Nishizawa, T. Fukuda, H. Kimura, H. Nojiri, K. Kaneko, and S. Maekawa, Phys. Rev. Lett. **82**, 4328 (1999).
  - <sup>22</sup> S. Ishihara, M. Yamanaka, N. Nagaosa, Phys. Rev. B **56**, 686 (1997).
  - <sup>23</sup> R. Maezono, S. Ishihara and N. Nagaosa, Phys. Rev. B **57**, R13993 (1998).
  - <sup>24</sup> R. Maezono, S. Ishihara and N. Nagaosa, Phys. Rev. B **58**, 11583 (1998).
  - <sup>25</sup> E.O. Wollan, and W.C. Koehler, Phys. Rev. **100**, 545 (1955).
  - <sup>26</sup> K. I. Kugel, and D. I. Khomskii, ZhETF Pis. Red. **15**, 629 (1972). (JETP Lett. **15**, 446 (1972)); D. I. Khomskii, and K. I. Kugel, Sol. Stat. Comm. **13**, 763 (1973).
  - <sup>27</sup> S. Ishihara, J. Inoue, and S. Maekawa, Physica C **263**, 130 (1996), and Phys. Rev. B **55**, 8280 (1997).
  - <sup>28</sup> H. Kawano, R. Kajimoto, H. Yoshizawa, Y. Tomioka, H. Kuwahara, and Y. Tokura, Phys. Rev. Lett. **78**, 4253 (1997).
  - <sup>29</sup> H. Kuwahara, T. Okuda, Y. Tomioka, T. Kimura, A. Asamitsu, and Y. Tokura, Mat. Res. Soc. Sym. Proc. **494**, 83 (1998).
  - <sup>30</sup> Y. Moritomo, T. Akimoto, A. Nakamura, K. Ohoyama, and M. Ohashi, Phys. Rev. B **58**, 5544 (1998).
  - <sup>31</sup> H. Kuwahara, T. Okuda, Y. Tomioka, A. Asamitsu, and Y. Tokura, Phys. Rev. Lett. **82**, 4316 (1999).
  - <sup>32</sup> R. Kajimoto, H. Yoshizawa, H. Kawano, H. Kuwahara, Y. Tokura, K. Ohoyama, and M. Ohashi, preprint (cond-mat/990233).
  - <sup>33</sup> G. Matsumoto, J. Phys. Soc. Jpn. **29**, 606 (1970).
  - <sup>34</sup> H. Fujioka, M. Kubota, K. Hitota, H. Yoshizawa, Y. Moritomo, and Y. Endoh, J. Phys. Chem. Solids, in press (cond-mat/9902253).
  - <sup>35</sup> R. Maezono and N. Nagaosa, preprint (cond-mat/9904427).
  - <sup>36</sup> E. Fradkin, in *Field Theories of Condensed Matter Systems*, Addison-Wesley Publishing Company (1991).
  - <sup>37</sup> J. B. Goodenough, Phys. Rev. **100**, 564 (1955).
  - <sup>38</sup> D.N. Argyriou, J.F. Mitchell, J.B. Goodenough, O. Chmaissem, S. Short, and J.D. Jorgensen, Phys. Rev. Lett. **76**, 1568 (1997).
  - <sup>39</sup> D.N. Argyriou, J.F. Mitchell, C.D. Potter, S.D. Bader, R. Kleb and J.D. Jorgensen, Phys. Rev. B. **55**, R11965 (1997).
  - <sup>40</sup> T. G. Perring, G. Appeli, Y. Moritomo, and Y. Tokura, Phys. Rev. Lett. **78**, 3197 (1997).
  - <sup>41</sup> K. Hirota, Y. Endoh, Y. Moritomo, Y. Maruyama, and A. Nakamura, preprint submitted to PRB Rapid; K. Hirota, Y. Moritomo, H. Fujioka, M. Kubota, H. Yoshizawa, and Y. Endoh, J. Phys. Soc. Jpn. **67**, 3380 (1998).
  - <sup>42</sup> T. Kimura, Y. Tomioka, A. Asamitsu, and Y. Tokura, preprint.
  - <sup>43</sup> M. Kubota, H. Fujioka, K. Ohoyama, K. Hirota, Y. Moritomo, H. Yoshizawa, and Y. Endoh, preprint submitted to J. Phys. Chem. Solids (1998).
  - <sup>44</sup> Recent experiments with  $x > 0.5$  confirms that this prediction of the global topology is consistent with the observation, except some instability of the incommensurate phase seen for  $x \sim 0.8$  (J.F. Mitchell, private communication, 1999).

- <sup>45</sup> H. Kawano, R. Kajimoto, H. Yoshizawa, Y. Tomioka, H. Kuwahara, and Y. Tokura, preprint (cond-mat/9808286).
- <sup>46</sup> H. Y. Hwang, P. Dai, S-W. Cheong, G. Aeppli, D.A. Tennant, and H.A. Mook, Phys. Rev. Lett. **80**, 1316 (1998).
- <sup>47</sup> J.A. Fernandez-Baca, P. Dai, H.Y. Hwang, C. Kloc, and S-W. Cheong, Phys. Rev. Lett. **80**, 4012 (1998).
- <sup>48</sup> P. Dai, H.Y. Hwang, J. Zhang, J.A. Fernandez-Baca, S-W. Cheong, C. Kloc, Y. Tomioka, and Y. Tokura, preprint (cond-mat/9904372).
- <sup>49</sup> J. W. Lynn, talk in FSRC (1999).
- <sup>50</sup> I. Solov'yev, N. Hamada, and K. Terakura, Phys. Rev. Lett. **76**, 4825 (1996).
- <sup>51</sup> K. Hirota, N. Kaneko, A. Nishizawa, and Y. Endoh, J. Phys. Soc. Jpn. **65**, 3736 (1996).
- <sup>52</sup> H. Yoshizawa, H. Kawano, J. A. Fernandez-Baca, H. Kuwahara, Y. Tokura, Phys. Rev. B **58**, R571 (1998).
- <sup>53</sup> R. Maezono and N. Nagaosa, preprint (cond-mat/9901076).
- <sup>54</sup> Y. Endoh and K. Hirota, J. Phys. Soc. Jpn. **66**, 2264 (1997).
- <sup>55</sup> M.C. Martin, G. Shirane, Y. Endoh, K. Hirota, Y. Moritomo and Y. Tokura, Phys. Rev. B **53**, R14285 (1996).
- <sup>56</sup> N. Nagaosa, in preparation.
- <sup>57</sup> G. Khaliullin and R. Kilian, preprint (cond-mat/9904316).
- <sup>58</sup> G. D. Mahan, in *Many-Particle Physics, 2nd ed.*, Chap. 4 (Plenum Press, New York, 1990).
- <sup>59</sup> K. I. Kugel and D. I. Khomskii, Sov. Phys. JETP **52**(3), 501 (1981).
- <sup>60</sup> M. Quijada, J. Černe, J.R. Simpson, H.D. Drew, K.H. Ahn, A.J. Millis, R. Shreekala, R. Ramesh, M. Rajeswari, and T. Venkatesan, Phys. Rev. B **58**, 16093 (1998).